HEFAT2007
5th International Conference on Heat Transfer, Fluid Mechanics and Thermodynamics
Sun City, South Africa
Paper number: KJ2

LIQUID WALL FILM FORMATION IN STEAM PIPING IN NUCLEAR PLANT

J. Katolicky[1], M. Jicha[1]*, R. Mares[2]
*Author for correspondence
[1] Faculty of Mechanical Engineering,
Brno University of Technology,
Technicka 2, 61669 Brno, Czech Republic,
Email: jicha@fme.vutbr.cz
[2] West Bohemia University
Univerzitni 8, 30614 Plzen, Czech Republic

ABSTRACT

A numerical investigation is carried out for turbulent droplet-laden flow of saturated steam produced in a steam generator (SG) that feeds steam turbine (ST) through a long and multi-bend steam piping. The main purpose of the study is to analyze deposition of droplets that form a wall film in the piping system. Two tasks were performed: parametric study of the deposition in 90° elbows and the deposition in a more complex piping system. This system starts with outlets from the steam generator with five mouthpieces leading to a collector pipe and connecting the steam piping leading to a steam turbine. Results of the simulations show where droplets deposit and where a liquid separator should be placed to drain away the water film and to avoid droplets from entering the steam turbine. Dynamic temporal development of the film is presented showing mutual impact of gravity and entrainment by the co-flowing steam.

INTRODUCTION

Saturated steam that is produced in steam generators (SG) in a nuclear plant passes through a perforated plate, which serves as a droplets separator. However the elimination of droplets never reaches 100% and the steam leaving the SG always contains a certain percentage of droplets. Water content of the steam must be eliminated from the steam before the steam enters the ST as droplets could damage turbine blades. Droplets that "fly" with the steam, depending on their size either impinge on the wall or separate by gravitation and form a wall film. Also turbulent dispersion contributes to the wall film formation, but only very small droplets having very small Stokes number are subject to this motion. Several devices are used to remove droplets from the steam, such as for example, a water film cutter placed on the inner steam piping wall in an appropriate position. It is not a trivial task to predict a right position where the cutter should be placed. Any experiments in a real steam piping are practically impossible and physical modeling that would retain all features of a real piping is difficult if not impossible as well. The situation is aggravated by the fact that the geometrical configurations of the steam piping differ from plant to plant and also in the same plant there are several SG and steam piping. The process of water separation thus depends on the individual steam piping layout.

Deposition of droplets on the pipe wall can be solved either using different empirical formulas for deposited mass flow rate or by the solution of film equations. In the deposition process, droplets in the gas core may follow the turbulent gas fluctuations depending on their size. Therefore some kind of turbulent diffusion from regions of high droplet concentrations into the regions with smaller concentration is possible if the droplets are small enough. The deposition of droplets on the walls is defined as a process of transfer of droplets from the gas bulk flow to the wall leading to an increase of the film wall thickness. If the core is turbulent there is in any case droplet deposition on the wall.

Historically there are several empirical attempts in the literature to model the deposition process. Among several empirical correlations we have to mention that of Zajchik et al. [1] based on the turbulence fluctuation theory in dispersed flows, correlation of Matsuura et al. [2], Paleev and Filippovich [3], Sugawara [4], Nigmatulin [5], Katto [6], Owen and Hewitt [7], Lopes and Ducler [8] or Schadel et al. [9]. All correlations have limited validity for different combination of gas and liquid, for pressure range, Reynolds number or film and droplet void fraction.

PROBLEM DESCRIPTION AND FLOW CONFIGURATION

Parametric study was performed in five different elbow orientations marked as Var.1 to Var.5 - see Figure 1. In all scenarios there are identical straight portions of the piping: 0.85m upstream and 3.7m downstream the elbow. Middle radius of the bend is 0.75m. Diameter of the piping is 0.425m. Mass steam flow rate was chosen 452 ton/hour. Steam moisture was taken 0.25%, which corresponds to the droplet mass flow 0.313 $kg.s^{-1}$. Physical parameters are in Tab.1.

Tab.1 Physical parameters of saturated steam and water

Pressure of saturated steam [MPa]	4.71
Temperature [°C]	260.2
Specific mass of saturated steam [kg.m^{-3}]	23.81
Specific mass of water [kg.m^{-3}]	783.4
Dynamic viscosity of steam [Pa.s]	1.886x10^{-5}
Dynamic viscosity of water [Pa.s]	101.613x10^{-6}
Surface tension of water [Nm^{-1}]	0.0236

In the complex piping system the saturated steam leaves the SG through five mouthpieces that lead steam into a collector pipe. The mouthpieces have each an inner diameter 0.24m and a length 0.9m. The collector pipe has a length 8.61m and an inner diameter 0.425m. Steam piping - see Figure 2 - has a total length 17m and the pipe diameter is 0.425m.

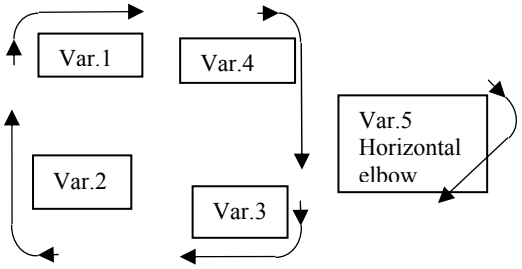

Figure 1 Orientation of elbows for parametric study

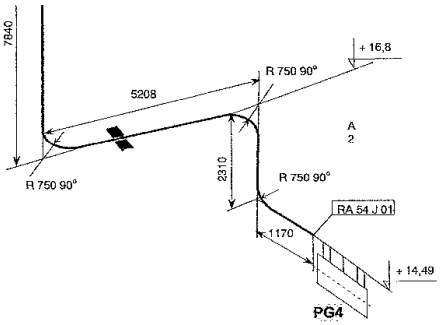

Figure 2 Piping system

Size spectrum of droplets entering the pipe is assumed in the range from 100 μm to 1000 μm with the MMD (Mass Median Diameter) $D_{0.5}$ = 320 μm. Many particle size distributions that occur in nature have been found to follow the Gaussian or normal distribution law with the logarithm of the particle diameter – called the log-normal distribution

$$f(D^3) = \frac{1}{\sqrt{2\pi}Ds_g}\exp\left[\frac{1}{2s_g^2}\left(\ln D - \ln \overline{D}_{vg}\right)^2\right]$$

where D in the function f(D) equals *ln*D, $\overline{D}_{vg}$ is the geometric mass or volume mean drop diameter $D_{0.5}$ and s_g is the geometrical standard deviation.

Droplets that are entrained from SG and carried by saturated steam are assumed in 10 size classes evenly distributed by mass so that in each size class there is 10% of mass or volume of liquid droplets - see Tab.2 - calculated from the above log-normal distribution. The entire size spectrum is assigned in 10 positions uniformly distributed in the entrance cross section of each of the five mouthpieces connecting SG and the collector pipe.

Tab.2 Droplets size classes in [μm]

Size class	Lower limit	Upper limit	Mean value
1	100	168	134
2	168	210	189
3	210	245	227,5
4	245	280	262,5
5	280	320	300
6	320	365	342,5
7	365	412	388,5
8	412	480	446
9	480	597	538,5
10	597	1000	798,5

NUMERICAL MODELING OF THE CONTINUUM PHASE

Numerical modeling of particle-laden turbulent flow was performed using the Reynolds-averaged Navier-Stokes (RANS) equations:

$$\frac{\partial \overline{u_i}}{\partial t} + \frac{\partial}{\partial x_j}\left(\overline{u_i}\,\overline{u_j}\right) = -\frac{1}{\rho}\frac{\partial \overline{p}}{\partial x_i} + \nu\frac{\partial^2 \overline{u_i}}{\partial x_j \partial x_j} - \frac{\partial \tau_{ij}}{\partial x_j} + S^p$$

where $\overline{u}_i$, $\overline{u}_j$ are time-averaged velocity components, t is time, p is pressure, x_j are coordinates, τ_{ij} is shear stress, ρ is density and S^p is a source from the particulate phase. CFD code StarCD was used for the solution. Equations were closed by the k-ω model of turbulence according to Wilcox in which it is easier to prescribe the boundary conditions. Variable ω is the specific dissipation rate and is proportional to ε/k, where k is turbulent kinetic energy and ε is its rate of dissipation.

NUMERICAL MODELING OF THE DISPERSED PHASE

The transport of droplets is handled by the Lagrangian approach in which the primary steam flow is calculated by using RANS models together with eddy interaction models. Here we use the most commonly used model by Gosman and Ioannides [10], a stochastic approach where individual particles are allowed to interact successively with discrete eddies, each having length, velocity and lifetime characteristic scales obtained from the primary flow calculation results.

DROPLETS DEPOSITION AND LIQUID FILM FORMATION

The liquid wall film model is based on the work of Bai and Gosman [11]. The dynamic model is used here that accounts for transfer processes within the continuous phase with assumptions:

• Film is thin enough for the boundary layer approximation to apply

• Velocity profile across the film is parabolic and the temperature profile is piece-wise linear
• Film will spread across a wall face with constant thickness
• Flow is laminar
• Analysis is transient
• No mass transfer by condensation

Solution of the film conservation equations is obtained by solving the mass conservation equation using the "thin film" assumptions

$$\frac{\partial}{\partial t}(\rho_l \delta) + \frac{\partial}{\partial x_i}(\rho_l \delta \bar{u}_l) = \dot{m}_l$$

where ρ_l is the film density, δ the film thickness and $\bar{u}_l$ the depth-averaged film velocity. The term $\dot{m}_l$ represents a source/sink for the film mass transfer rate per unit wall area. The depth-averaged film velocity $\bar{u}_l$ is obtained from momentum conservation equation by assuming that the unsteady and convective terms in the momentum equation can be neglected. A balance of forces on a liquid film of volume V_{lf} yields:

$$0 = \left[-V_{lf} \left(\frac{\partial p}{\partial x_i} - \rho \mathbf{F}_i \right) \right] + \mathbf{S}_d + \mathbf{S}_b (\tau_f - \tau_w)$$

where $\mathbf{S}_d$ is the momentum contribution from impinging droplets, $\mathbf{F}_i$ the body force per unit mass, τ_f the shear stress exerted at the fluid-film interface by the fluid, and τ_w the shear stress at the wall. $\mathbf{S}_b$, the wall area vector for the area wetted by the film, is taken to be equal to the cell face area at the wall. The pressure term p includes both the continuous phase pressure and the impingement pressure due to droplets hitting the film. Above equation is solved together with the equations for τ_w and τ_f to yield the expressions for coefficients of the parabolic velocity profile within the wall film.

NUMERICAL ASPECTS OF THE CALCULATIONS

In the parametric study, droplets were ascribed in 26 locations evenly distributed in the cross section of the inlet to the pipes so that each location represents the same area. Number of droplets parcels was chosen 300/second, the total number of parcels per second was 78 000 (26 locations, in each location 10 size classes and 300 parcels in each size class). The whole calculation represents 4 seconds of the actual time and during this time in total 312 000 parcels were released.

The calculations of the complex piping system flow field started with preliminary calculations to obtain flow distribution at the entrance from SG to five mouthpieces according to pressure losses in the individual mouthpieces and the collector pipe. In the preliminary calculations, the total pressure of 4.71 MPa in the SG was ascribed as the inlet condition and at the exit from the collector pipe the outlet condition was specified. As a result, flow distribution at the inlet to the individual mouthpieces was obtained. This distribution was then used as the inlet boundary conditions for the calculations of the whole piping system. Similarly to the parametric study, droplets were assigned in the entrance to the mouthpieces in 26 locations uniformly distributed in each cross section. In each of the locations, 10 size classes were assigned and 100 parcels were defined per second. Numerical mesh contained 3,800,000 cells, and the time step was 0.0005s. One time step required at the beginning of the calculations 200s of the real computing time, and then it decreased to 60s.

RESULTS AND THEIR DISCUSSION

Results of the parametric study of the scenarios Var.1 to Var.5 are shown in the form of the time development of the wall film thickness in 5 locations depicted in the Figure 3. The film thickness is analyzed in 8 individual segments S1 to S8 along the pipe cross section perimeter from which a mean of the sum of neighboring segments 1+8, 2+3, 4+5 a 6+7 is drawn (figure 4). Plots of the time development in selected locations E2 and E5 are in figure 5. In the location E1 the film thickness doesn't show any difference between individual times, the segments and the scenario.

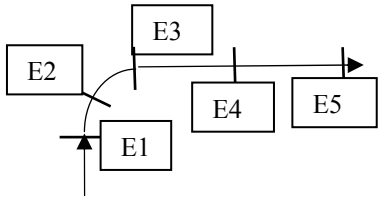

Figure 3 Individual locations E

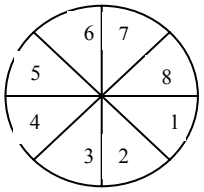

Figure 4 Individual segments S

The minimum, almost constant thickness, approximately 15μm is formed shortly after the inlet to the pipe, where the steam flow is not disturbed by aggregate turbulent structures and the film is formed almost solely by turbulent diffusion. In the following locations the film thickness increases mainly by impact and reaches values approximately 80 μm to 120 μm. A stable oscillating film thickness is formed within 1 to 1.5 second after the beginning of the process. Very interesting is the time delay of the film formation in the segments 2+3 (more pronounced in more distant locations) where the film is formed also by liquid flowing down from the upper segments of the pipe cross section (segments 2 and 3 are on the surface with the smaller radius). From the location E2 on, the film thickness begins significantly stratify for individual segments which is caused by the droplets impact. In all variants except the var.1 the maximum film thickness is in segments 6 and 7, i.e. in the upper part of the elbow corresponding to the outer radius. In the var.1 the film thickness in the upper segments 6 and 7 is comparable with the thickness in the lower segments 2 and 3, to where the film flows down along the side part of the elbow due to gravitation. In general, one can say that in the more distant locations behind the elbow, except Var.1, the minimum film thickness is in the side and lower segments of the cross

section. Oscillating character of the time development of the film thickness results from droplets impact and thus from the permanent breakup of the film. The film thickness in all variants reaches an equilibrium state where the thickness is around 100 μm to 120μm. It can be concluded that the total film formation is not significantly influenced by gravitation but rather by the character of the flow field in the elbow and just behind it. Gravitation influences rather the local arrangement of the film in the individual segments of the pipe cross section.

Results of the calculations of the complex piping system are presented in the form of the liquid film thickness and the film velocity fields developing along the piping system in fig. 6. We can make an overall impression on how the film develops in a global manner. The film continuously develops and is drained away from the piping systems. Most of the liquid flows in the "bottom" part of the pipe, i.e. through the segments S2+3. It is interesting to inspect the film thickness in times 2s and 5s, where we can see how the film flows downward between these times from the segment 4 towards the "bottom" segments 2 and 3 causing the increase in the film thickness.

CONCLUSIONS

From the parametric study the following conclusions can be made:

1. Different orientation of the elbow does not have practically any impact on the thickness of the wall film and thus on the amount of the liquid leaving the pipe. Even though the film forms on different pipe surface segments, gravitation makes always the film to flow into lower parts of the cross section given a sufficient distance the steam flows. Velocity of the film that flows down due to gravitation is sufficiently high to displace the film along the pipe surface. It is likely advantageous to have a certain straight portion of the pipe behind the elbow to determine the down flowing.
2. Wall film is mostly affected by the droplets impaction in which the whole droplets size spectrum participates. Turbulent dispersion itself influences only very small droplets (here the value of Stokes number should be known in the correlation with for example the Kolmogorov length scale) and in comparison with the impaction is negligible.

ACKNOWLEDGMENT

Financial support from the projects No. 101/03/0632 of the Czech Grant Agency and No. 1H134S001 from the Ministry of Industry and Trade are gratefully acknowledged.

REFERENCES

[1] Zajchik, L. I., Nigmatulin, B. I. and Alipchenko, V.M., 1998, Droplet deposition and film atomization in gas-liquid annular flow, 3rd International conference on multiphase flow, ICMF 98, Lyon, France

[2] Matsuura, K., Kataoka, I and Serizawa, A., 1995, Prediction of droplet deposition rate based on Lagrangian simulation of droplet behavior, Proceedings of the 3rd JSME/ASME Joint International conference on Nuclear Engineering, Kyoto, Japan, vol.1, pp. 105-109

[3] Paleev, I. I., Filippovich, B.S., 1966, Phenomena of liquid transfer in two-phase dispersed annular flow, Int. J. Heat Mass Transfer, vol.9, p.1089

[4] Sugawara, S., 1990, Droplet deposition and entrainment modeling based on the three-fluid model, Nuclear Engineering and Design, vol. 122, pp. 67-84

[5] Nigmatulin, B.I., 1982, Heat and mass transfer and force interaction in annular-dispersed two-phase flow, 7th Int. Heat Transfer Conference, Munich, pp.337-342

[6] Katto, Y., 1984, Prediction of critical heat flux for annular flow in tubes taking into account of the critical liquid film thickness concept, Int. J. Heat Mass Transfer, vol.27, pp.883-890

[7] Owen, G.D. and Hewitt, G.F., 1987, An improved annular two-phase flow model, 3rd BHRA Int. Conference on Multiphase Flow, The Hague

[8] Lopes, J.C.B. and Ducler, A.E., 1986, Droplet entrainment in vertical annular flow and its contribution to momentum transfer, AIChE Journal, vol. 32, pp. 1500-1515

[9] Schadel, S.A., Leman, G.W., Binder, J.L. and Hanratty, T.J., 1990, Rates of atomization and deposition in vertical annular flow, Int. J. Multiphase Flow, vol. 16, pp. 363-374.

[10] Gosman, A.D. and Ioannides, E., 1981, Aspects of computer simulation of liquid fueled combustors, Paper AIAA-81-0323, 19th Aerospace Science Meeting, St. Louis, MO.

[11] Bai, C., and Gosman, A.D., 1995, Development of methodology for spray impingement simulation, SAE Technical Paper Series 950283.

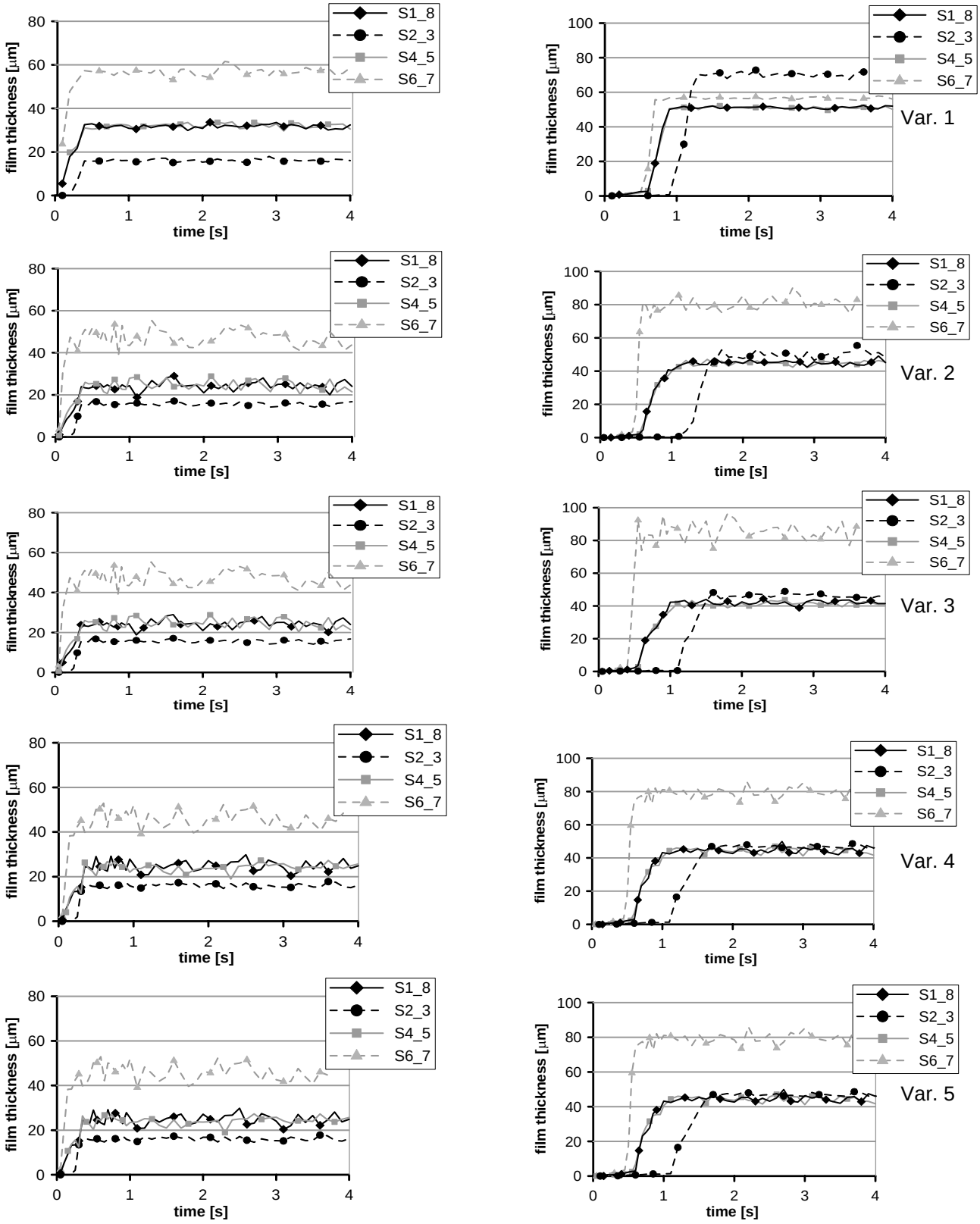

Figure 5 Time development of wall film thickness for position E2 (left) and E5 (right) in five variants of elbow geometries

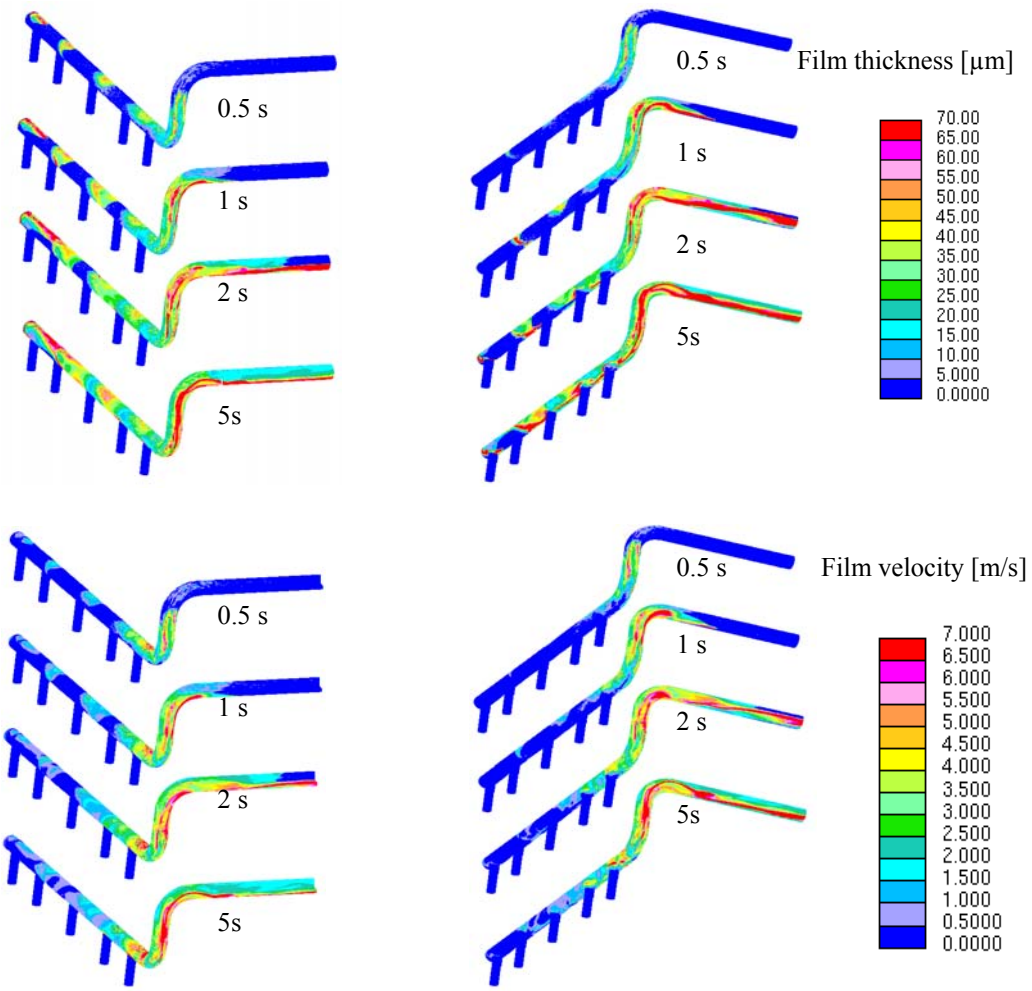

Figure 6 Film thickness and film velocity in the whole piping system as function of time